The Journal of Neuroscience, June 1, 2002, 22(11):4456–4467

Developmental Regulation of Small-Conductance Ca^{2+}-Activated K^+ Channel Expression and Function in Rat Purkinje Neurons

Lorenzo A. Cingolani,[1] Marco Gymnopoulos,[1] Anna Boccaccio,[1] Martin Stocker,[1,2] and Paola Pedarzani[1,3]

[1]Max-Planck-Institute for Experimental Medicine, 37075 Göttingen, Germany, and [2]Wellcome Laboratory for Molecular Pharmacology, Department of Pharmacology, and [3]Department of Physiology, University College London, London WC1E 6BT, United Kingdom

Calcium transients play an important role in the early and later phases of differentiation and maturation of single neurons and neuronal networks. Small-conductance calcium-activated potassium channels of the SK type modulate membrane excitability and are important determinants of the firing properties of central neurons. Increases in the intracellular calcium concentration activate SK channels, leading to a hyperpolarization of the membrane potential, which in turn reduces the calcium inflow into the cell. This feedback mechanism is ideally suited to regulate the spatiotemporal occurrence of calcium transients. However, the role of SK channels in neuronal development has not been addressed so far. We have concentrated on the ontogenesis and function of SK channels in the developing rat cerebellum, focusing particularly on Purkinje neurons.

Electrophysiological recordings combined with specific pharmacological tools have revealed for the first time the presence of an afterhyperpolarizing current (I_{AHP}) in immature Purkinje cells in rat cerebellar slices. The channel subunits underlying this current were identified as SK2 and localized by *in situ* hybridization and subunit-specific antibodies. Their expression level was shown to be high at birth and subsequently to decline during the first 3 weeks of postnatal life, both at the mRNA and protein levels. This developmental regulation was tightly correlated with the expression of I_{AHP} and the prominent role of SK2 channels in shaping the spontaneous firing pattern in young, but not in adult, Purkinje neurons. These results provide the first evidence of the developmental regulation and function of SK channels in central neurons.

Key words: SK channel; afterhyperpolarization; apamin; calcium-activated potassium current; development; Purkinje neurons

Neuronal development involves dramatic changes in both the morphology and excitable membrane properties of the differentiating neurons. In particular, calcium (Ca^{2+}) transients with various spatiotemporal features have been shown to be involved in the early and later phases of differentiation and maturation of single neurons and neuronal networks (for reviews, see Spitzer, 1994; O'Donovan, 1999; Ben-Ari, 2001). Work performed on *Xenopus* spinal neurons has revealed that potassium (K^+) currents, mainly of the voltage-dependent type, play a pivotal role in the maturation of the action potential and of the neuronal firing behavior (Spitzer and Ribera, 1998; Ribera, 1999). Small-conductance Ca^{2+}-activated K^+ channels (Kohler et al., 1996; Joiner et al., 1997) regulate the firing properties of neurons in the CNS (Sah, 1996). Given their high sensitivity to Ca^{2+}, they are ideally suited to regulate the spatiotemporal features of Ca^{2+} transients by a feedback mechanism, but their role in neuronal development has not been addressed so far.

The rat cerebellum is an ideal system for studying the functional impact of different ion channels during neuronal development, because it is immature at birth and develops rapidly in the first weeks of postnatal life. Purkinje cells provide the sole cerebellar efferent pathway. Their differentiation involves complex interaction between intrinsic and extrinsic programs (Hatten and Heintz, 1995; Goldowitz and Hamre, 1998) and can be divided into three general phases, which are completed within the first 3 weeks of postnatal development, and during which Purkinje neurons organize themselves into a discrete monolayer and progressively develop their typical, elaborated dendritic tree and synaptic contacts (Uzman, 1960; Altman, 1972; Altman and Bayer, 1997). Spontaneous activity *in vivo* can be observed in rat Purkinje cells already at postnatal day (P) 1–2, and it matures progressively in terms of frequency and regularity of the firing pattern over the first 3 postnatal weeks, reaching values comparable with the adult ones (Woodward et al., 1969; Latham and Paul, 1971; Crepel, 1972).

Intracellular Ca^{2+} transients play a major signaling role throughout postnatal development, as well as in adult Purkinje cells (Tank et al., 1988; Gruol et al., 1992; Miyakawa et al., 1992; Eilers et al., 1996). A number of studies have addressed the developmental regulation of components essential for Ca^{2+} signaling in Purkinje neurons, such as Ca^{2+} channels (Regan, 1991; Gruol et al., 1992; Falk et al., 1999), pumps (Takei et al., 1992; Strehler and Zacharias, 2001), Ca^{2+} binding proteins (Iacopino et al., 1990; Solbach and Celio, 1991; Ni et al., 1992; Milosevic and

Received Jan. 8, 2002; revised March 5, 2002; accepted March 11, 2002.

This work was supported by grants from the Deutsche Forschungsgemeinschaft Sonderforschungsbereich 406, Project C8 (M.S., P.P.) and the Human Frontier Science Program (P.P.). M.S. is a Wellcome Trust Senior Research Fellow. We thank D. D'hoedt, K. Hentrich, M. E. Rubio, A. Thalhammer, and F. Varoqueaux for assistance and advice. We thank Rüdiger W. Veh for technical advice on the purification of antibodies. We are very grateful to Walter Stühmer for his generous support, and to David A. Brown for useful discussion. The excellent technical assistance of B. Scheufler, R. Schubert, and the personnel of the animal facility at the Max-Planck-Institute for Experimental Medicine is acknowledged.

Correspondence should be addressed to Dr. Paola Pedarzani, Department of Physiology, University College London, Gower Street, London WC1E 6BT, UK, E-mail: p.pedarzani@ucl.ac.uk; or Dr. Martin Stocker, Wellcome Laboratory for Molecular Pharmacology, University College London, Gower Street, London WC1E 6BT, UK, E-mail: m.stocker@ucl.ac.uk.

Zecevic, 1998; Spilker et al., 2000), and Ca^{2+} buffering capacity (Fierro and Llano, 1996). Additionally, the role of large-conductance Ca^{2+}- and voltage-dependent K^+ channels (BK type) in the maturation of Purkinje cells has been studied extensively in cultured preparations (Muller et al., 1998, 2000; Muller and Yool, 1998).

This study focuses on a family of small-conductance Ca^{2+}-activated K^+ channels, the SK channels, that are ideally suited to modulate calcium transients. By combining eletrophysiological recordings in rat cerebellar slices with *in situ* hybridization and immunohistochemistry, we have demonstrated for the first time the presence of an afterhyperpolarizing current (I_{AHP}) and the expression of the underlying apamin-sensitive Ca^{2+}-activated SK channels in Purkinje neurons at early developmental stages. Furthermore, this study presents the first evidence of a tight developmental regulation of SK channel expression and provides evidence for a prominent and specific role of these channels in the regulation of the firing properties of Purkinje cells during the first weeks of postnatal development.

MATERIALS AND METHODS

In situ *hybridization. In situ* hybridization was performed on sagittal brain sections (10–16 μm) from three male Wistar rats of different breeding pairs at the following postnatal ages: P1, P3, P6, P12, P24, and P60 (P1 being the day of birth), using ^{35}S-labeled antisense and sense oligonucleotide probes according to the procedure described in detail by Stocker and Pedarzani (2000). The sequences of subunit-specific sense and antisense oligonucleotides used in this study were identical to those used and described previously (Stocker and Pedarzani, 2000).

The following control experiments were performed. First, adjacent sections were hybridized with labeled sense oligonucleotides to determine the general nonspecific background. Second, the specificity of the probes was controlled by performing competition experiments with a 500-fold excess unlabeled oligonucleotide included in the hybridization mixture. This control experiment did not result in detectable signal at any developmental stage (data not shown). Finally, the oligonucleotide probes selected for this study had been used previously to analyze the distribution of SK channel transcripts in the adult rat brain (see Fig. 1, *P60 panels*) (Stocker and Pedarzani, 2000). On adult brain sections, identical hybridization patterns had been obtained with a second set of oligonucleotide probes for every SK channel subunit. This indicated that these independent probes recognized the same gene product, ruling out the possibility of spurious cross-reactivity (Stocker and Pedarzani, 2000).

Antibody production and purification. Subunit specific antibodies against the amino- (anti-NSK2) and the C- (anti-CSK2) terminus of the SK2 subunit (GenBank accession no. U69882) were generated. The N-terminal sequence of SK2, corresponding to amino acid 23–83, was amplified by PCR and cloned into the bacterial expression vector pGEX-2T. After induction, the glutathione *S*-transferase-NSK2 fusion protein was purified by standard procedures and lyophilized. Polyclonal rabbit antisera were generated by a standard protocol for anti-NSK2 at Biogenes (Berlin, Germany).

The anti-NSK2 antibody was affinity purified using the pET-NSK2 fusion protein, comprising the same channel region used to generate the antibody inserted into the pET32 (Novagen, Madison, WI). All constructs were confirmed by sequencing. The pET-NSK2 fusion protein was overexpressed in *Escherichia coli* (BL21-DE3), purified using Ni-NTA agarose (Quiagen, Hilden, Germany) following the manufacturer's recommendations, and adsorbed to nitrocellulose membrane (Schleicher und Schuell, Dassel, Germany). After blocking (5% low-fat milk powder in PBS, 2 hr), the membrane was incubated with the antiserum at 4°C overnight. Anti-NSK2 was eluted with an acidic buffer, pH 2.5, containing 0.2 M glycine, 150 mM NaCl, and 1 mg/ml bovine serum albumin (BSA) and subsequently desalted (NAP10 columns, Amersham Biosciences, Freiburg, Germany).

Western blot. Human embryonic kidney 293 (HEK-293) cells were transiently transfected with the rat SK2 subunit cloned into pcDNA3 (Invitrogen, San Diego, CA) using Lipofectamine 2000 (Invitrogen). After 24 hr, cells were extracted at 4°C with a buffer containing 10 mM Tris-HCl, 150 mM NaCl, 1 mM DTT, 6.5% SDS, at pH 6.8, supplemented with a protease inhibitor mixture (Complete Mini tablet; Roche Diagnostics), and proteins were solubilized by sonication. The protein concentration of the soluble fraction was determined with the BCA Protein Assay Kit (Pierce, Rockford, IL). Proteins (2–5 μg) were separated on a 10% SDS polyacrylamide gel and transferred to a nitrocellulose membrane (Hybond-ECL, Amersham Biosciences). Western blotting was performed using the ECL chemoluminescent system (Amersham Biosciences). Blocking was performed in 5% low-fat milk powder and 5% normal goat serum (NGS) in PBS plus 0.1% Tween 20 for 30 min. The purified anti-NSK2 and the anti-CSK2 antibodies were used at a dilution of 1:500. Anti-rabbit horseradish peroxidase-conjugated secondary antibody (Bio-Rad, Hercules, CA) was used at a dilution of 1:5000. Blots were exposed to film for 0.5–2 min.

Controls were performed in parallel where either the primary antibody was omitted or purified anti-NSK2 antibody was preincubated with pET-NSK2 (10–20 μg/ml, 8–16 hr, 4°C).

Immunofluorescence on HEK-293 cells expressing SK channels. Stably transfected cells were plated onto poly-lysine-coated coverslips for 48–72 hr, washed in PBS, and fixed with 4% paraformaldehyde (10 min). After permeabilization (0.2% Triton X-100) and washing, cells were preblocked (10% calf serum, 3% BSA, 37°C, 30 min). Next, the purified anti-NSK2 or the anti-CSK2 antibodies were applied (1:500, 1 hr, 37°C). After repeated washes with PBS, the secondary FITC-conjugated donkey anti-rabbit antibody (1:500, Amersham Biosciences, Arlington Heights, IL) was applied (30 min, 37°C). Coverslips were mounted and immunostaining was visualized with a fluorescence microscope (Axioscope, Zeiss), and pictures were taken with a CCD camera (SPOT, Diagnostic Instruments, Inc.).

Immunohistochemistry. Male Wistar rats were anesthetized with a mixture of ketamine HCl (Ketaset, 100 mg/ml; Fort Dodge Laboratories Inc.) and xylazine (Rompum, 20 mg/ml; Miles, Elkhart, IN) at 0.1 ml/100 gm of body weight. The animals were transcardially perfused with 4% paraformaldehyde in 0.12 M phosphate buffer, pH 7.35. After perfusion, brains were removed, fixed for an additional hour at 4°C, and rinsed three times in PBS.

Sagittal sections (50 μm thick) were cut in cold PBS using a Vibratome (Leica VT1000S, Nussloch, Germany) and incubated for 1 hr in PBS containing 10% NGS, followed by an overnight incubation at 4°C with the primary antibody (anti-NSK2 1:500, diluted in PBS containing 2% NGS). The next morning the free-floating sections were washed and incubated first with the biotinylated goat anti-rabbit IgG (1:200, 1 hr, room temperature) and then with avidin–biotin complex system (ABC, Vectastain Elite, Vector Laboratories, Burlingame, CA) for 1 hr at room temperature. Peroxidase activity was revealed by 2–9 min incubations at room temperature with 3,3′-diaminobenzidine as a chromogen (Vector Laboratories). In controls, sections were incubated without primary antibody, or purified anti-NSK2 antibody was treated with fusion protein as described above. The second antibody (anti-CSK2) was used in parallel for all experiments using the anti-NSK2 antibody and gave similar results, thereby confirming the specificity of the staining obtained with the anti-NSK2 antibody. Sections were analyzed with a Zeiss Axioscope microscope, and pictures were taken with a CCD camera (SPOT, Diagnostic Instruments, Inc.). For each stage, sections from two animals were analyzed.

Slice preparation and electrophysiology. Sagittal cerebellar slices (250–300 μm thick) of the vermis region were prepared from male Wistar rats (12 and 50–60 d old) with a Vibratome (Leica VT1000S) and subsequently incubated in a humidified interface chamber or in a submerged chamber at room temperature for ≥1 hr. Tight-seal whole-cell recordings were obtained from the somata of Purkinje cells under visual control. Patch electrodes (4–7 MΩ) were filled with an intracellular solution containing (in mM): 135 potassium gluconate, 10 KCl, 10 HEPES, 2 Na_2-ATP, 0.4 Na_3-GTP, 1 $MgCl_2$ (pH 7.2–7.3 with KOH). In experiments in which BAPTA (10 mM) was added to the intracellular solution, the concentration of potassium gluconate was reduced to 110 mM to maintain constant osmolarity. Current-clamp recordings were performed also in the cell-attached and perforated-patch configurations. For the perforated-patch measurements, electrodes (4–5 MΩ) were back-filled with amphotericin B (350 μg/ml). Recordings were performed in a submerged chamber with a constant flow of artificial CSF (ACSF, 2 ml/min) at room temperature (21–24°C). ACSF contained (in mM): 125 NaCl, 1.25 KCl, 2.5 $CaCl_2$, 1.5 $MgCl_2$, 1.25 KH_2PO_4, 25 $NaHCO_3$, 16 D-glucose, and was bubbled with carbogen (95% O_2/5% CO_2). Drugs were applied in the bath solution. In voltage-clamp recordings, tetrodotoxin (TTX; 0.5 μM) and tetraethylammonium (TEA; 1 mM) or alternatively penitrem A (10 μM) were added to the superfusing ACSF. Pur-

kinje cells were depolarized from a holding potential of −50 mV to values ranging from −8 to +40 mV for a period of 100–300 msec every 30 sec to induce unclamped Ca^{2+} spikes. Subsequently the membrane potential was stepped back to −50 mV to record afterhyperpolarization (AHP) currents as Ca^{2+}-activated tail currents. In Purkinje cells the unclamped calcium spikes present characteristic regenerative all-or-none properties. Given the tight dependence of I_{AHP} from the amount of calcium influx (see Results and Fig. 6*C*,*D*), particular care was taken in maintaining the number of calcium spikes constant before and after drug applications. Series resistance was monitored at regular intervals throughout the recording, and only measurements with a stable series resistance ≤25 MΩ were included in this study. No series resistance compensation and no corrections for liquid junction potentials were made. Only cells with a stable resting membrane potential (±1 mV) throughout the experiment were included in the analysis. Data were generated and acquired using an EPC9 amplifier (HEKA, Lambrecht Germany) and the Pulse software (HEKA). In voltage-clamp experiments, data were filtered at 1 kHz and sampled at 4 kHz; in current-clamp experiments, data were filtered at 0.4–3.3 kHz and sampled at 1.6–13.3 kHz.

Analysis was performed using the programs Pulsefit (HEKA), Igor Pro 3.01 (Wave Metrics), Excel (Microsoft), and InStat (GraphPad Software). All data are presented as mean ± SEM; statistical differences were determined by the Student's *t* test with $\alpha < 0.05$ taken as the level of significance. In current-clamp recordings the burst frequency (number of bursts per second) and the frequency of the single spikes (inverse of the interspike interval) were calculated over a period of 2 min for every cell tested. Coefficients of variation (CVs) were obtained by dividing the SD by the mean interspike interval. When pharmacological tests were performed, frequencies and CVs were calculated immediately before application and after reaching the full effect of the applied drug.

TEA, potassium gluconate, Na_2-ATP, Na_3-GTP, dimethylsulfoxide, and amphotericin B were obtained from Sigma (Münich, Germany); TTX and penitrem A were obtained from Alomone Laboratories (Jerusalem, Israel); apamin and iberiotoxin were obtained from Latoxan (Rosans, France); 1-ethyl-2-benzimidazolinone (1-EBIO) was obtained from Tocris Cookson (Bristol, UK); BAPTA was obtained from Molecular Probes (Eugene, OR); all other salts and chemicals were obtained from Merck (Darmstadt, Germany).

RESULTS

SK transcripts in Purkinje neurons during postnatal development

Ca^{2+}-activated K^+ channels of the SK type are widely expressed in a number of CNS neurons (Stocker and Pedarzani, 2000), where they mediate apamin-sensitive I_{AHP} that play an important role in shaping neuronal firing patterns (Sah, 1996; Stocker et al., 1999; Pedarzani et al., 2000; Wolfart et al., 2001). Given their high Ca^{2+} sensitivity [cloned SK2 channels: EC_{50} ~0.3 μM (Xia et al., 1998); native small-conductance Ca^{2+}-activated K^+ channels in hippocampal neurons: EC_{50} ~0.6 μM (Hirschberg et al., 1999)], SK channels are activated even by small increases in the intracellular Ca^{2+} concentration and cause a hyperpolarization of the membrane potential. The hyperpolarization reduces Ca^{2+} influx, making of SK channels an ideally suited feedback system to regulate the spatiotemporal occurrence of calcium transients.

Bearing in mind the pivotal role played by Ca^{2+} signals in neuronal differentiation and maturation and the special features of SK channels, we focused on the ontogenesis of SK channels and AHP currents in rat Purkinje neurons *in situ* to investigate the role of these channels in the development of Purkinje cell excitability and firing properties. Understanding the contribution of SK channels to the development of the signaling properties of Purkinje cells requires information about their expression and localization in these cells. Therefore, we performed a detailed *in situ* hybridization analysis of the expression of the three SK subunit mRNAs (SK1, SK2, and SK3) in Purkinje cells. We selected five stages of postnatal development, covering the first 3 postnatal weeks, during which Purkinje cells reach their mature phenotype and connectivity: P1 (corresponding to the day of birth), P3, P6, P12, and P24, as well as one additional time point at adult age (P60). SK1 and SK3 mRNAs were not detectable in Purkinje cells at any developmental stage analyzed (data not shown). Conversely, the SK2 transcript, encoding the SK subunit with the highest sensitivity to the bee-venom toxin apamin, was abundantly expressed in Purkinje neurons throughout the cerebellum already at P1 (Fig. 1). The expression of SK2 mRNA can be seen as a thick white layer of silver grains in the dark-field picture (Fig. 1, *P1*, *left panel*). At birth, Purkinje cells are still organized in a multilayered band in the cerebellar anlage (Uzman, 1960), as is visible in the light-field picture (Fig. 1, *P1*, *right panel*). During the first postnatal days, Purkinje cells organize themselves into a discrete monolayer located between the internal granule layer and the molecular layer in the developing cerebellar cortex (Altman and Bayer, 1997). At this stage, the expression of the SK2 subunit mRNA persisted at high levels, as is evident particularly in the light-field pictures (*P3*, *P6*, and *P12*, *right panels*), where the dark silver grains are easily visible over the Purkinje cell somata. These stages were followed by a clear decline in the SK2 expression level, as is evident from the dark-field pictures as well as from the reduced number of silver grains localized over the Purkinje neurons in the light-field pictures when going from P12 to P24 (Fig. 1), and finally leading to the very low levels observed in the adult (Fig. 1) (see also Stocker and Pedarzani, 2000).

Localization of SK channel subunits in Purkinje neurons at different developmental stages

To investigate the localization of SK2 channels in the cerebellum, we generated rabbit polyclonal antibodies against amino- and C-terminal sequences of the rat SK2 subunit, which show no significant homology to the corresponding regions in the SK1 and SK3 subunits. To demonstrate the specificity of the generated antibodies, Western analysis of HEK-293 cells transiently transfected with the SK2 subunit was performed. Figure 2 shows that the C-terminal antibody anti-CSK2 (Fig. 2*A*, *lane 1*), as well as the affinity-purified amino-terminal antibody anti-NSK2 (Fig. 2*A*, *lane 3*) recognized a band corresponding to a molecular weight of 59 kDa, which is in good agreement with the molecular weight predicted from the amino acidic sequence of the SK2 subunit (63 kDa). A second higher molecular weight band (>110 kDa) could be identified (Fig. 2*A*, *lanes 1*, *3*). That both antibodies recognized the lower and the higher molecular weight bands, that none of these bands could be identified in nontransfected HEK-293 cells (Fig. 2*A*, *lanes 2*, *4*), and that no bands could be detected when the anti-NSK2 antibody was preincubated with the corresponding fusion protein demonstrated that the raised antibodies were specific. Furthermore, these results indicate that the higher molecular weight band corresponds to an aggregate of SK2 subunits.

Next, we performed a set of immunocytochemical experiments on HEK-293 cell lines expressing SK1, SK2, or SK3 to demonstrate the subunit specificity of the anti-CSK2 and anti-NSK2 antibodies. In Figure 2, *B* and *C*, immunofluorescence signals show the binding of the anti-CSK2 and the affinity-purified anti-NSK2 antibody to cells expressing the SK2 channel. A membrane localization was visible with both antibodies. The same antibodies did not generate any signals when applied to nontransfected cells or to cell lines expressing SK1 or SK3 channels (data not shown), thereby demonstrating their subunit specificity. In Figure 2*D*, cells expressing SK2 channels were labeled with a fluorescent

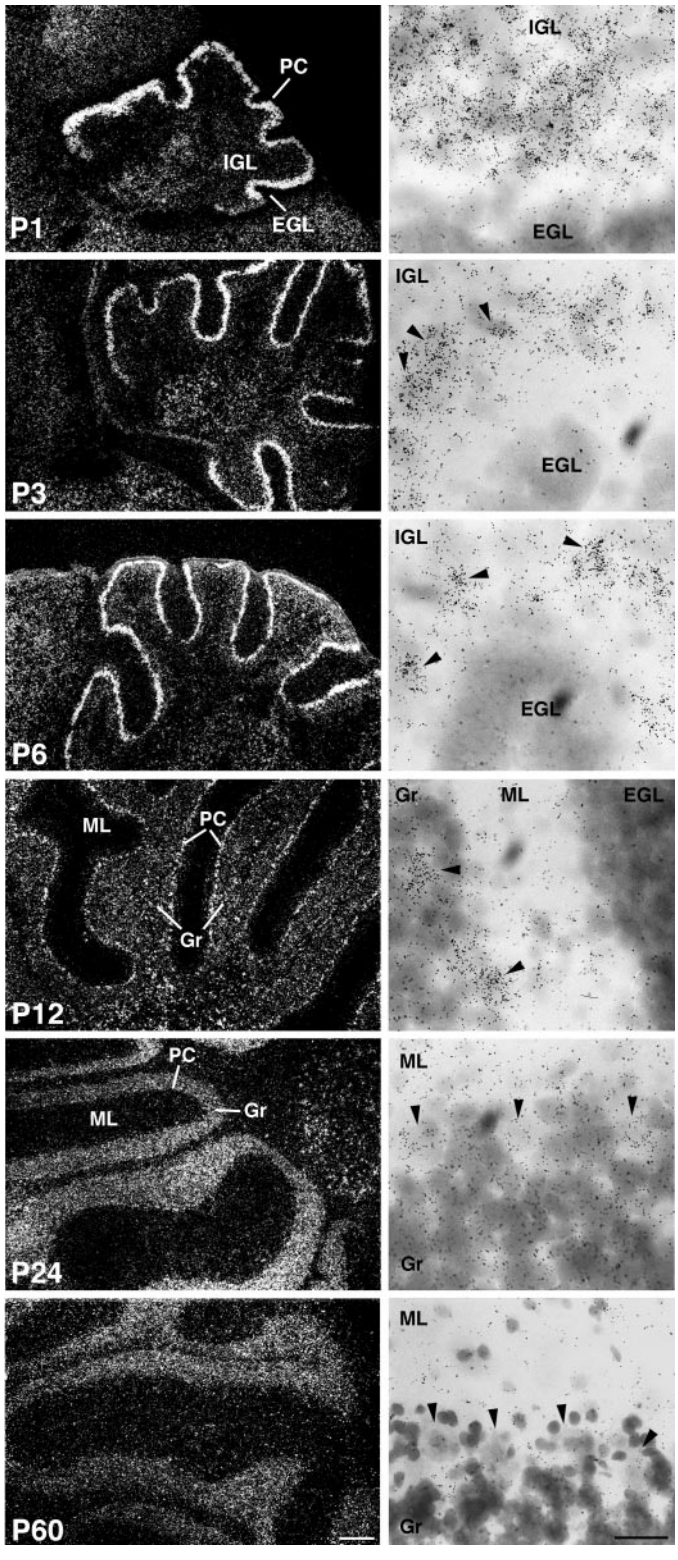

Figure 1. The expression level of SK2 mRNA is developmentally regulated in the rat cerebellum. *In situ* hybridization was performed on sagittal sections at different developmental stages (*P1*, *P3*, *P6*, *P12*, *P24*, and *P60*) with SK2-specific oligonucleotides. Sections were coated with photoemulsion and exposed for 3 months. The probe for SK2 strongly labeled Purkinje cells (*PC*) from P1 to P12. The silver grains can be identified as white signals in the layer labeled as PC in the dark-field photomicrographs on the *left*. Light-field photomicrographs show cresyl violet-counterstained Purkinje cell neurons at high magnification (*right panels*), where the SK2 signal is visible as clusters of black dots over the cell nuclei. At P1, Purkinje neurons are organized in a multilayered band located between the internal and external granule layer and already display a high level of SK2 mRNA. At P3, P6, and P12, Purkinje cells are organized in a discrete monolayer, and *arrowheads* point to some of the silver grain clusters over Purkinje cell nuclei. Conversely, at P24 and P60 the signal observed in the dark-field photomicrographs (*left panels*) is attributable to a moderate level of expression of SK2 transcript in granule cells. The SK2 signal on single Purkinje cells (*arrowheads* in *P24* and *P60*, *right panels*) is below the threshold limit of detection. *EGL*, External granule layer; *Gr*, granule cells; *IGL*, internal granule layer; *ML*, molecular layer; *PC*, Purkinje cells. Scale bars: dark-field, *left panels*, 250 μm; light-field, *right panels*, 25 μm.

derivative of apamin (apamin-Alexa488). The apamin-binding was performed on nonfixed and nonpermeabilized cells and confirmed the membrane localization of the SK2 subunits. No binding could be observed on empty HEK-293 cells.

The immunopurified anti-NSK2 antibody gave rise to a specific, strong DAB immunoreaction in Purkinje cells at P12 (Fig. 2*E*,*G*,*I*) showing the presence of the SK2 subunit. Both omission of primary antiserum (data not shown) and preabsorption of anti-NSK2 antibodies with the fusion protein (Fig. 2*F*) resulted in the lack of DAB immunoreaction, confirming the specificity of the signal. Nearly all Purkinje cells at P12 showed strong immunoreactivity (Fig. 2*G*), whereas only a few scattered Purkinje cells at P60 showed a weak staining (Fig. 2*H*). Higher resolution revealed a localization of the SK2 immunoreactivity in the somata and main dendritic branches of P12 Purkinje neurons (Fig. 2*I*). Figure 2*J* shows the weak staining of one mature Purkinje cells (P60), whereas the neighboring cells, indicated by *arrows*, were devoid of any immunoreactivity. The second antibody generated against a peptide derived from the C-terminal region of SK2 (anti-CSK2) yielded similar results (data not shown).

Altogether it can be concluded that the expression of SK2 transcripts (Fig. 1) as well as of SK2 channel subunits (Fig. 2*G–J*) shows a progressive reduction during the first 3 weeks of postnatal development, leading to a complete downregulation at adult age in Purkinje neurons. Therefore, the data obtained by *in situ* hybridization and immunohistochemistry demonstrate unequivocally that the expression of SK2 channel subunits in cerebellar Purkinje cells is developmentally regulated.

Impact of SK channel activity on the firing pattern of developing Purkinje cells

The evidence that we obtained of a developmental regulation of the SK channel expression at the mRNA and protein level led us to hypothesize that these channels might play a differential role in regulating the firing properties of Purkinje neurons at different developmental stages.

To test this hypothesis, we investigated the firing patterns of Purkinje neurons from 12-d-old rats, because P12 is a central day in the decisive period of the second to third week of postnatal development (see introductory remarks), when intrinsic properties and synaptic connectivity of Purkinje neurons reach their final stage of maturation (Altman and Bayer, 1997). Additionally, according to our *in situ* hybridization (Fig. 1) and immunohistochemistry data (Fig. 2), P12 is the later stage when a very homogeneous, high expression level of SK2 transcript and channel protein can still be observed when compared with P24 or adult Purkinje neurons.

Purkinje neurons at P12 presented three different patterns of spontaneous firing activity (Fig. 3). The first pattern, observed in the majority of the cells (~50%), displayed a rhythmic bursting

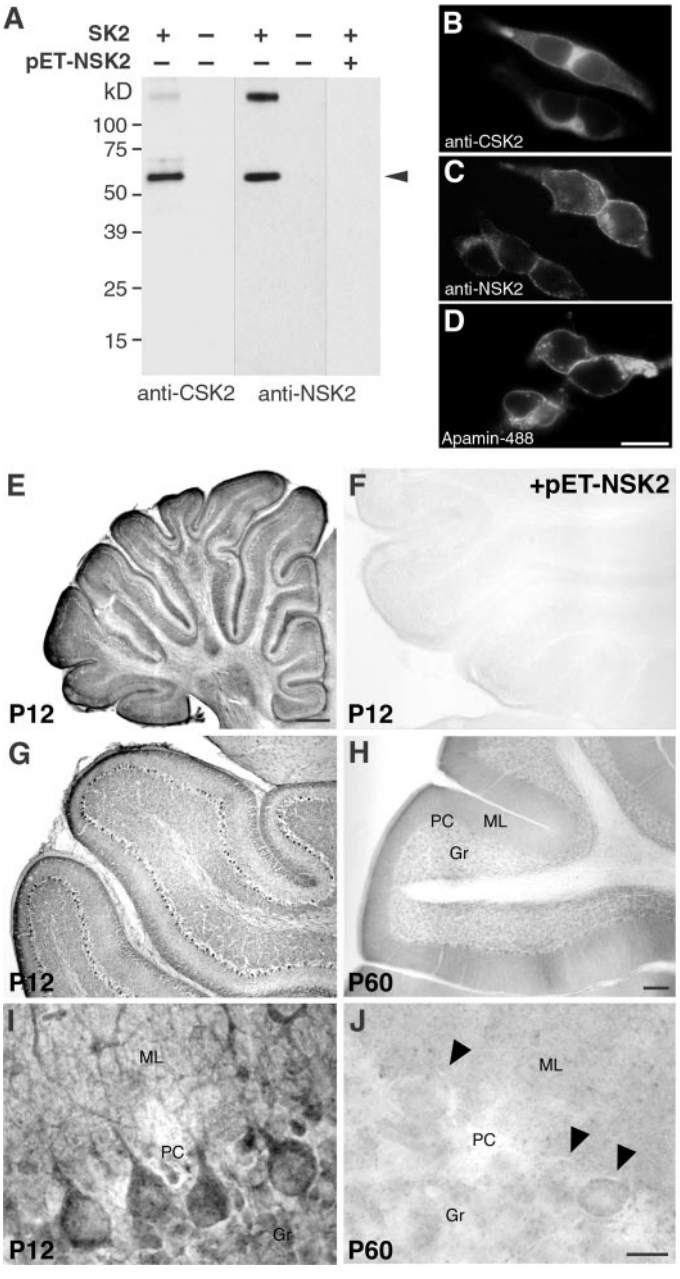

Figure 2. The expression of SK2 protein is developmentally regulated in Purkinje neurons, as shown by immunohistochemistry with SK2-specific antibodies. *A*, Western blot on SK2 channel subunits expressed in HEK-293 cells and characterized with anti-CSK2 and affinity-purified anti-NSK2 antibody. *Arrowheads* indicate the bands corresponding to the SK2 channel subunit (*lanes 1*, *3*). There are no bands visible in fractions from cells that do not express SK2 channel subunits (*lanes 2*, *4*). No bands are detected after preadsorption of the primary antibody with the antigen (*lane 5*), demonstrating that the high molecular band corresponds to an aggregate of SK2 channel subunits. *B*, *C*, Immunofluorescence of HEK-293 cells transfected with SK2, showing a specific staining with both the anti-CSK2 and the anti-NSK2 antibodies. *D*, Labeling of membrane standing SK2 channels in transfected HEK-293 cells with a fluorescent derivative of apamin (apamin-Alexa488). *E–J*, Light-microscopy micrographs showing the immunohistochemical reactions of the affinity-purified anti-NSK2 antibody in the cerebellum at P12 and P60. In *F*, no staining is visible with preadsorbed antibodies (*+pET-NSK2*). In *G* and *H*, low-magnification views of the cerebellum show strong SK2 signals on the majority of Purkinje neurons at P12 (*G*), but only very weak ones on a few scattered Purkinje neurons on sections from adult rats (*H*, *P60*). In *I* and *J*, at a cellular level of resolution, Purkinje neurons show a strong SK2 signal on the somata and the dendritic stem at P12 (*I*), but not at P60 (*J*). In *J*, three Purkinje cells are indicated by *arrowheads*. One of them presents a light stain by anti-NSK2. This was observed in sporadic cases, but the level of staining at P60 was always lower than the one observed at earlier developmental stages (*I*). *Gr*, Granule cells; *ML*, molecular layer; *PC*, Purkinje cells. Scale bars: *B, C, D*, 20 μm; *E*, 0.5 mm; *F, G, H*, 150 μm; *I*, *J*, 20 μm.

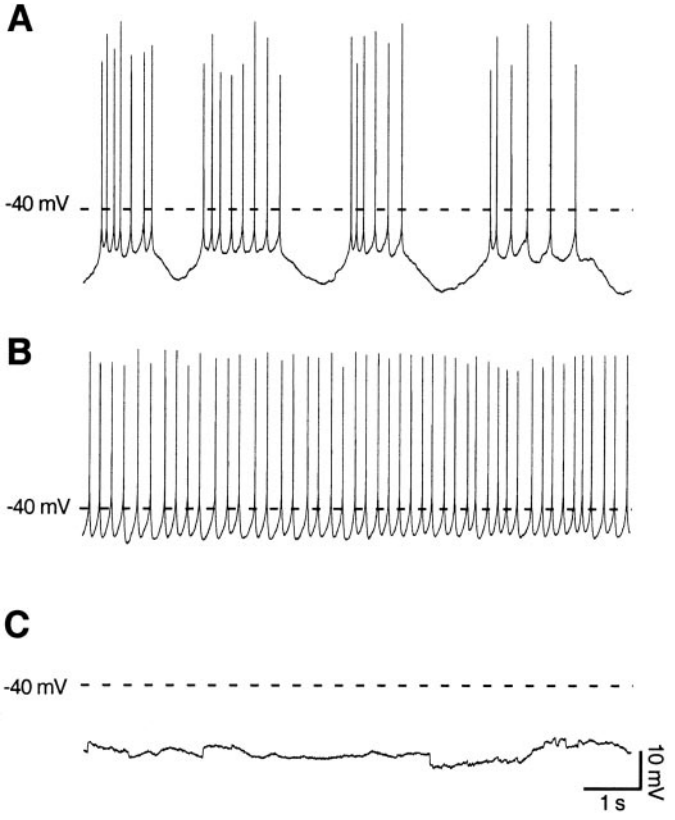

Figure 3. Purkinje cells present different spontaneous firing patterns at P12. *A*, Fifty percent of the Purkinje cells presented a pattern of spontaneous activity characterized by rhythmic bursts of action potentials at P12. The mean burst frequency was 0.36 ± 0.03 Hz, the burst duration was 1.6 ± 0.2 sec, and the interburst intervals were 1.8 ± 0.2 sec (n = 32). *B*, Approximately 30% of the Purkinje cells showed a sustained tonic firing of single spikes with an average frequency of 4.4 ± 0.7 Hz and a CV of 0.24 ± 0.03 (n = 20). *C*, The remaining 20% of the cells did not present any spontaneous firing (silent cells) and displayed an average membrane resting potential of −57 ± 2 mV (n = 12). All traces displayed were recorded in the whole-cell configuration, with no steady current injected. The *dashed line* corresponds to a membrane potential of −40 mV. Calibration is the same for all three traces.

behavior, with a mean burst frequency of 0.36 ± 0.03 Hz, a burst duration of 1.6 ± 0.2 sec, and interburst intervals of 1.8 ± 0.2 sec (n = 32) (Fig. 3*A*). The second pattern, observed in ~30% of the cells, showed a sustained tonic firing of single spikes with an average frequency of 4.4 ± 0.7 Hz (n = 20) (Fig. 3*B*). Finally, the third pattern found in the remaining 20% of the cells did not present any spontaneous firing (silent cells) (Fig. 3*C*) and displayed an average membrane resting potential of −57 ± 2 mV (n = 12). This variability in the spontaneous firing patterns of the developing Purkinje neurons was not attributable to the recording conditions (whole-cell patch-clamp configuration), because we obtained nearly identical results also with perforated-patch recordings (57% of bursting, 29% of single spiking, and 14% of

silent cells; data not shown), where intracellular dialyzation does not occur. Moreover, the bursting and single spiking patterns were robust phenomena, because they did not substantially change by switching from the cell-attached to the whole-cell configuration in the same neuron ($n = 20$; data not shown).

Injection of steady depolarizing or hyperpolarizing currents could switch these spontaneous firing patterns in a consistent manner. Thus, injection of depolarizing current converted bursting cells into silent ones; a further depolarization led to tonic firing of single spikes in the same neuron. Steady depolarizing currents could also transform spontaneously silent cells into tonic firing ones. Conversely, cells presenting a sustained tonic firing of single spikes could be changed into silent ones by injection of hyperpolarizing current. Finally, in some cases tonic firing (2 of 8) or silent cells (1 of 5) could be converted into bursting ones by injecting steady hyperpolarizing currents (data not shown).

To elucidate the contribution of the SK channels to these different spontaneous firing patterns, we first tested the effect of apamin, a specific SK channel blocker (Strong, 1990), on rhythmically bursting Purkinje cells at P12 ($n = 4$). As shown in Figure 4, *A* and *B*, apamin (100 nM) produced two major effects on rhythmically bursting Purkinje cells: it increased the frequency of the action potentials within each burst (intraburst frequency) (Fig. 4*A*, *insets*, *B*) by more than twofold, and it clearly increased the frequency of the bursts (burst frequency) (Fig. 4*A*,*B*). A more detailed analysis of the bursting firing pattern revealed that apamin shortened the duration of each burst, without substantially affecting the length of the interburst intervals (Fig. 4*B*), and enhanced the Ca^{2+} spike terminating each burst (Fig. 4*A*, *inset*, *arrow*). Besides increasing the intraburst firing frequency, apamin decreased the regularity of the firing, as quantified by the change in the CV, corresponding to the SD normalized to the mean interspike interval (Fig. 4*B*).

When applied to tonically firing, single-spiking cells ($n = 5$), apamin (100 nM) reset the spontaneous firing pattern leading to the generation of spike doublets or bursts (Fig. 4*C*). In tonically firing Purkinje neurons, a detailed analysis revealed that apamin increased the overall firing frequency and even more prominently disrupted the regularity of the spike discharge as expressed by the increase in the CV (Fig. 4*D*).

Finally, in all silent Purkinje cells at P12, the application of apamin (100 nM) induced spontaneous firing of single spikes (Fig. 4*E*) without significantly affecting the resting membrane potential (-52 ± 2 mV before and -50 ± 2 mV after apamin application; $p = 0.65$). By contrast, in adult Purkinje neurons (P50–60), which in 56% of the cases did not display any spontaneous firing activity under our recording conditions, the same dose of apamin did not induce spontaneous firing ($n = 5$) (Fig. 4*F*), as observed instead at P12. Similarly, apamin did not change the firing pattern of the remaining 44% of adult Purkinje cells presenting sporadic single or complex spikes ($n = 4$; data not shown). Thus, suppression of the apamin-sensitive, voltage-independent SK channels strongly affects the spontaneous firing properties of developing (P12) but mature (P50–60) Purkinje neurons.

The observed effects on the spontaneous firing activity of young Purkinje cells are specific for the SK family of Ca^{2+}-activated K^+ channels, because suppression of the Ca^{2+}- and voltage-activated BK channel activity by the specific blocker iberiotoxin produced distinct effects on the firing patterns of Purkinje cells at P12. Iberiotoxin (50 nM) did not significantly affect burst duration in spontaneously bursting cells, and it decreased the firing frequency in tonically firing, single-spiking cells (data not shown), in contrast to the increase induced by apamin (Fig. 4*D*). Furthermore, suppression of the BK channel activity did not convert the firing pattern from tonic to bursting (data not shown), as shown for apamin in Figure 4*C*. On the basis of these results, we conclude that BK and SK channels regulate in different ways the spontaneous firing activity of developing Purkinje neurons.

The results we obtained with apamin strongly point to a critical involvement of SK channels in shaping the spontaneous firing pattern of young Purkinje neurons. In particular, blocking the channels with apamin favored or enhanced bursting. On the basis of this observation, enhancing, rather than suppressing, SK channel activity should induce an opposite effect, namely a transition from the bursting mode into a tonic, single-spike firing mode. As predicted, application of the SK channel enhancer 1-EBIO (100 μM) (Pedarzani et al., 2001) to spontaneously bursting Purkinje cells at P12 led to a tonic, single-spiking pattern (Fig. 5) ($n = 4$). In the presence of 1-EBIO, single spikes were fired at a low frequency (3.5 ± 0.6 Hz) and in a very regular manner (CV = 0.17 ± 0.05 compared with 0.24 ± 0.03 in spontaneously tonic, single-spiking neurons in the absence of 1-EBIO), each of them being followed by a pronounced afterhyperpolarization (Fig. 5, *middle panel*), a clear indication of an increased SK channel activity. Evidence that the 1-EBIO effect on the firing pattern was specifically induced by an enhancement of SK channel activity can be seen in Figure 5 (*bottom panel*), where the application of the selective SK channel blocker apamin reversed the effect of 1-EBIO completely.

Altogether, the results obtained on the firing activity of Purkinje neurons underscore the functional expression of SK channels and suggest that they play an important and specific role in modulating the spontaneous firing frequency and pattern of activity of developing Purkinje neurons.

A Ca^{2+}-activated current in developing Purkinje neurons

Given the effects of apamin and 1-EBIO on the spontaneous firing pattern of young Purkinje neurons, we were interested in characterizing the underlying SK-mediated current in these neurons. To record the SK-mediated I_{AHP} in P12 Purkinje cells, we adopted a protocol used previously successfully to isolate this current in hippocampal pyramidal neurons (Stocker et al., 1999). In particular, the membrane voltage was stepped from a holding potential of -50 mV to a depolarized potential (-8 to $+40$ mV) for 100–300 msec in the presence of the Na^+ channel blocker TTX (0.5 μM) and of the BK channel blockers TEA (1 mM) or penitrem A (10 μM) to elicit a robust Ca^{2+} influx corresponding to the generation of one or more all-or-none Ca^{2+} spikes (Fig. 6*A*,*B*, *insets*). Under these recording conditions, a tail current following the Ca^{2+} spikes (Fig. 6*A*) and resembling the I_{AHP} measured in hippocampal neurons could be observed. When three Ca^{2+} spikes were evoked (in 0.5 μM TTX + 10 μM penitrem A), the tail current presented an average amplitude of 446 ± 30 pA and a time constant of decay of 99 ± 13 msec ($n = 9$) (Fig. 6*A*). By contrast, mature Purkinje cells (P50–60) displayed no tail current under identical recording conditions ($n = 4$) (Fig. 6*B*).

As expected for the apamin-sensitive I_{AHP}, the amplitude and time course of the tail currents after the Ca^{2+} influx in P12 Purkinje neurons showed no voltage dependence (data not shown) but a clear correlation to the number of Ca^{2+} spikes triggered by the depolarizing pulse: peak amplitude and time constant of decay increased along with the number of Ca^{2+} spikes (Fig. 6*C*,*D*).

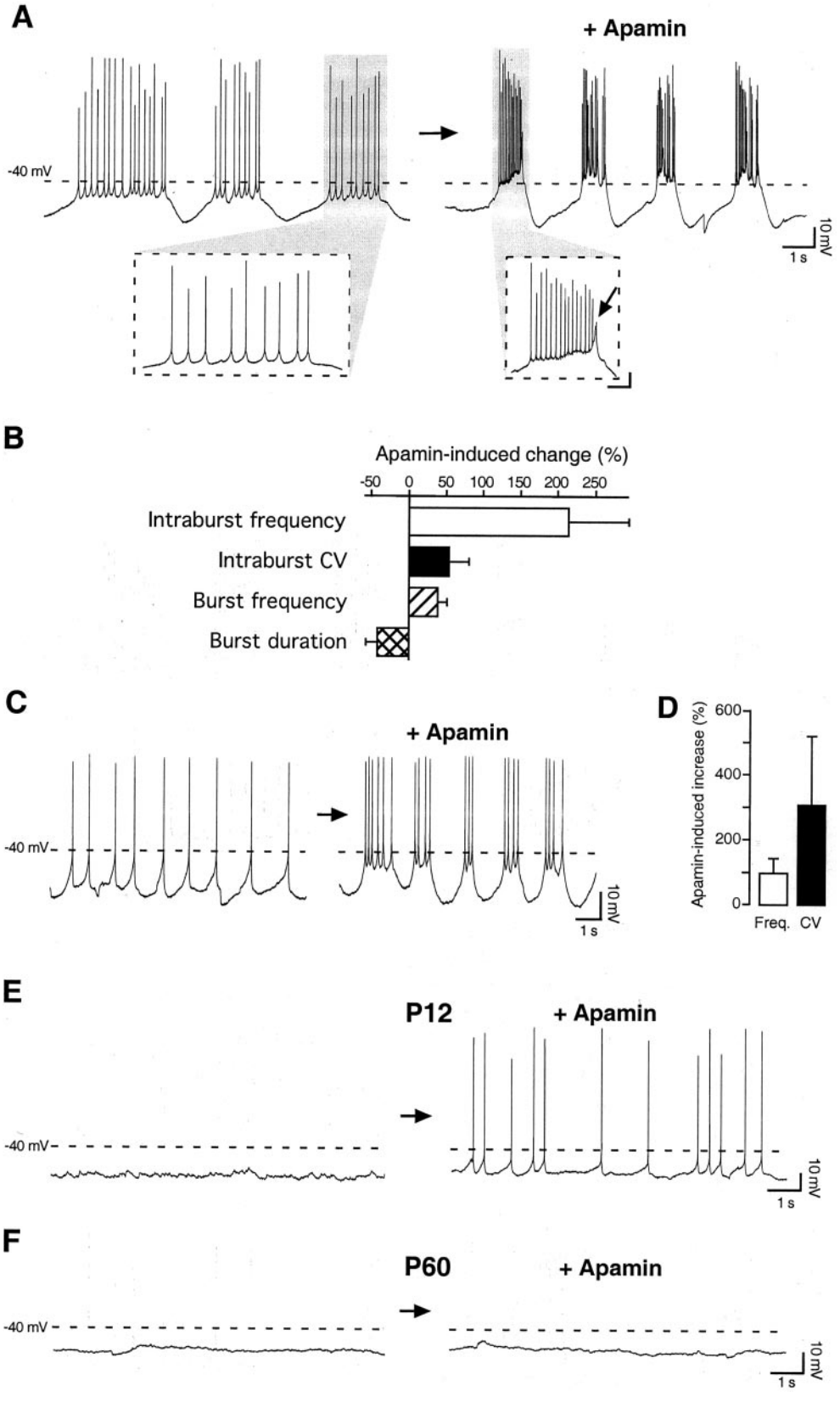

Figure 4. The SK channel blocker apamin modifies the spontaneous firing behavior of Purkinje neurons at P12 but not at adult age. *A*, When applied on spontaneously bursting Purkinje cells, apamin (100 nM) increased both the frequency of the action potentials within each burst (intraburst frequency) and the frequency of the bursts (burst frequency). Moreover, apamin shortened the duration of each burst and enhanced the Ca^{2+} spike terminating each burst (*inset*, *arrow*). Calibration in *inset*: 10 mV, 250 msec. *B*, Bar diagram summarizing the effects of apamin (100 nM) on spontaneously bursting Purkinje cells. The intraburst frequency was increased by 213 ± 81% ($n = 3$), and the burst frequency was increased by 37 ± 12% ($n = 4$), whereas the burst duration was reduced by 40 ± 15% ($n = 4$). Besides increasing the intraburst firing frequency, apamin decreased the regularity of the firing within each burst, as quantified by the increase in the CV by 54 ± 27% ($n = 3$). *C*, When applied to spontaneously single-spiking Purkinje cells, apamin (100 nM) favored the transition to a bursting firing pattern. *D*, Bar diagram summarizing the effect of apamin on single-spiking Purkinje cells. The overall firing frequency was increased by 97 ± 44%, and the CV was increased by 305 ± 213% ($n = 5$). *E*, At P12, apamin (100 nM) induced spontaneous firing of single spikes, without affecting the resting membrane potential (−52 ± 2 mV before and −50 ± 2 mV after apamin application; $p = 0.65$; $n = 4$). *F*, By contrast, apamin (100 nM) did not change the spontaneous firing behavior of silent Purkinje cells at adult age (*P60*). The *dashed line* in *A*, *C*, *E*, and *F* represents a membrane potential of −40 mV. No steady current was injected during these whole-cell current-clamp recordings.

The tight dependence of the tail current amplitude and decay time course on the number of evoked Ca^{2+} spikes provided a first indication of the Ca^{2+} dependence of the tail current. To show that the tail current was indeed Ca^{2+} activated, we performed three sets of experiments. First, removal of Ca^{2+} from the extracellular ACSF resulted in a full and reversible suppression of the tail current, concomitant with the disappearance of the Ca^{2+} spike (Fig. 6*E*,*H*). Second, application of 50 μM Cd^{2+} to block

voltage-gated Ca^{2+} channels potently and reversibly suppressed both Ca^{2+} spikes and tail currents (Fig. 6*F*,*H*). Finally, the addition of the fast Ca^{2+} chelator BAPTA (10 mM) to the pipette solution prevented the activation of the tail current during stimulation and intracellular [Ca^{2+}] increase. The tail currents could be observed only during the initial phase of whole-cell recordings with BAPTA (Fig. 6*G*, current trace 30 sec after breakthrough), and during dialyzation of the cell they declined irreversibly (Fig. 6*G*, current trace 4 min after breakthrough, and *H*). In parallel, we observed an increase in the number of Ca^{2+} spikes evoked by the same depolarizing pulse (data not shown).

Altogether, these results demonstrate that a Ca^{2+}-activated K^+ current of the AHP type (I_{AHP}) is indeed present in Purkinje neurons at postnatal day 12, but not in cells from adult animals.

The Ca^{2+}-activated current in P12 Purkinje neurons is sensitive to apamin and 1-EBIO

Besides being voltage independent and Ca^{2+} activated, in neocortical and hippocampal neurons I_{AHP} is specifically characterized by its sensitivity to the SK channel blocker apamin (Schwindt et al., 1992; Stocker et al., 1999) and to the SK channel enhancer 1-EBIO (Pedarzani et al., 2001). To test whether the tail current observed after Ca^{2+} spikes ultimately corresponds to I_{AHP}, we applied apamin to P12 Purkinje cells. Apamin (50 nM) strongly and irreversibly suppressed the Ca^{2+}-activated tail current (83 ± 4% inhibition; $n = 11$) (Fig. 7*A*). This effect was dose dependent, and the concentration of apamin producing a half-maximal suppression of the current (IC_{50}) was ~135 pM (Fig. 7*B*). This value is very close to the estimated sensitivity of recombinant homomultimeric SK2 channels (Kohler et al., 1996), suggesting that I_{AHP} is most probably mediated by homomultimeric SK2 channels in Purkinje neurons at P12. This assumption is supported by the exclusive expression of this subunit in young Purkinje neurons as detected by *in situ* hybridization (Fig. 1).

Recently, 1-EBIO has been introduced as a new pharmacological tool for the characterization of SK channels in heterologous and native systems and has been shown to enhance SK channel activity in a Ca^{2+}-dependent manner (Pedarzani et al., 2001). When applied to P12 Purkinje cells, 1-EBIO (100 μM) produced an increase in the peak amplitude of the Ca^{2+}-activated tail current (25 ± 5% increase; $n = 5$) (Fig. 7*C*,*D*). Additionally, it substantially prolonged the decay time course of the current (time constant of decay: 124 ± 15 msec before and 238 ± 25 msec after 1-EBIO application; $n = 5$; $p = 0.008$) (Fig. 7*C*,*D*). The increased amplitude and the slower deactivation of I_{AHP} induced by 1-EBIO were mostly reversible and resulted in a nearly twofold increase of the I_{AHP} charge transfer (168 ± 6% increase) (Fig. 7*D*). The complete block of the enhanced I_{AHP} by apamin demonstrated the specificity of the 1-EBIO effect on SK channels (data not shown).

The results obtained in voltage-clamp recordings allowed us to unequivocally identify the Ca^{2+}-dependent tail current observed in Purkinje neurons at P12 with I_{AHP}. A current with these features was not present in Purkinje cells from adult rats. These results are in agreement with the change in the expression level of SK2 subunit transcript and protein with age and with the observed effects of apamin on the firing patterns of P12 and adult Purkinje cells.

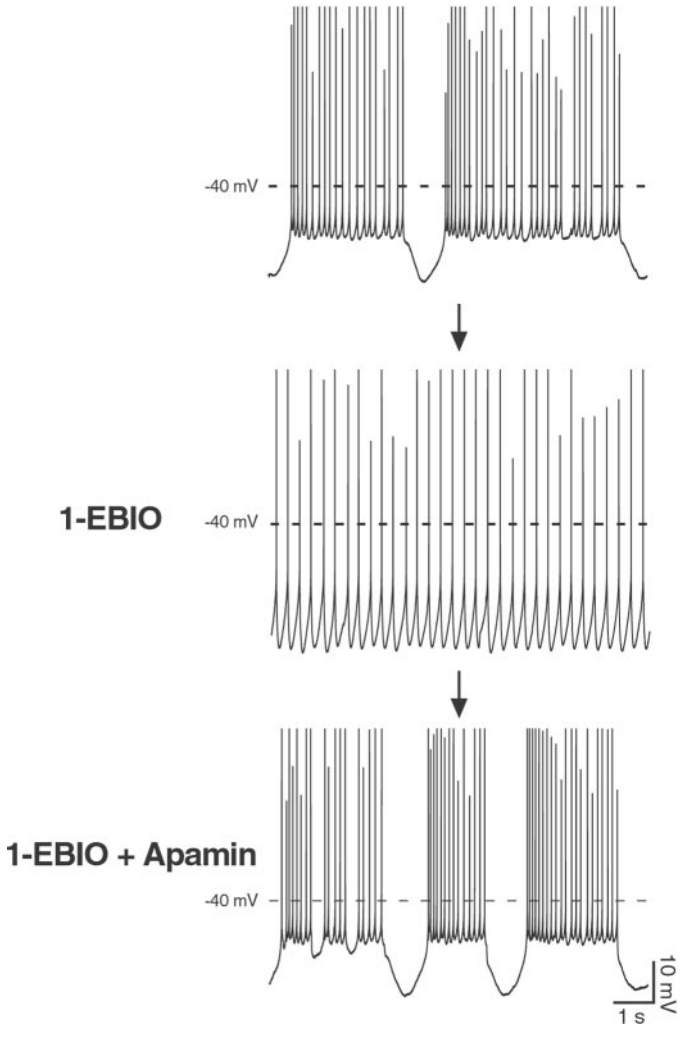

Figure 5. The SK channel enhancer 1-EBIO exerts an opposite effect to the blocker apamin on the spontaneous firing pattern of Purkinje neurons at P12. When applied to a spontaneously bursting Purkinje cell (*top panel*), 1-EBIO (100 μM) promoted the transition to a single-spiking pattern, with action potentials fired at a low frequency (3.5 ± 0.6 Hz) and in a very regular manner (CV = 0.17 ± 0.05; *middle panel*). Additionally, every action potential was followed by a pronounced afterhyperpolarization in the presence of 1-EBIO (*middle panel*), a clear indication of an increased SK channel activity. The application of apamin (100 nM) completely reversed the effect on the firing pattern induced by 1-EBIO and demonstrates unequivocally that 1-EBIO specifically enhanced SK channel activity (*bottom panel*). Similar results were obtained in four cells. All traces were recorded in the whole-cell configuration. Calibration is the same for all traces. Spike height was truncated for better resolution of the afterhyperpolarizations after single or bursts of action potentials.

DISCUSSION

This study provides the first molecular and functional characterization of the apamin-sensitive, voltage-independent Ca^{2+}-activated I_{AHP} in Purkinje neurons. The channel subunits underlying this current (SK2) were detected and localized by *in situ* hybridization and subunit-specific antibodies. A further novel and important finding is that the expression level of SK2 subunits is high at birth and subsequently declines during the first 3 weeks of postnatal life, both at the mRNA and at the protein level. This developmental regulation is tightly correlated with the expression of I_{AHP} and the prominent role of SK2 channels in shaping the spontaneous firing pattern in young (P12) but not in adult Purkinje neurons *in situ*.

Although a role for Ca^{2+}-activated K^+ currents in the regulation of the firing of Purkinje cells has been proposed (Llinas

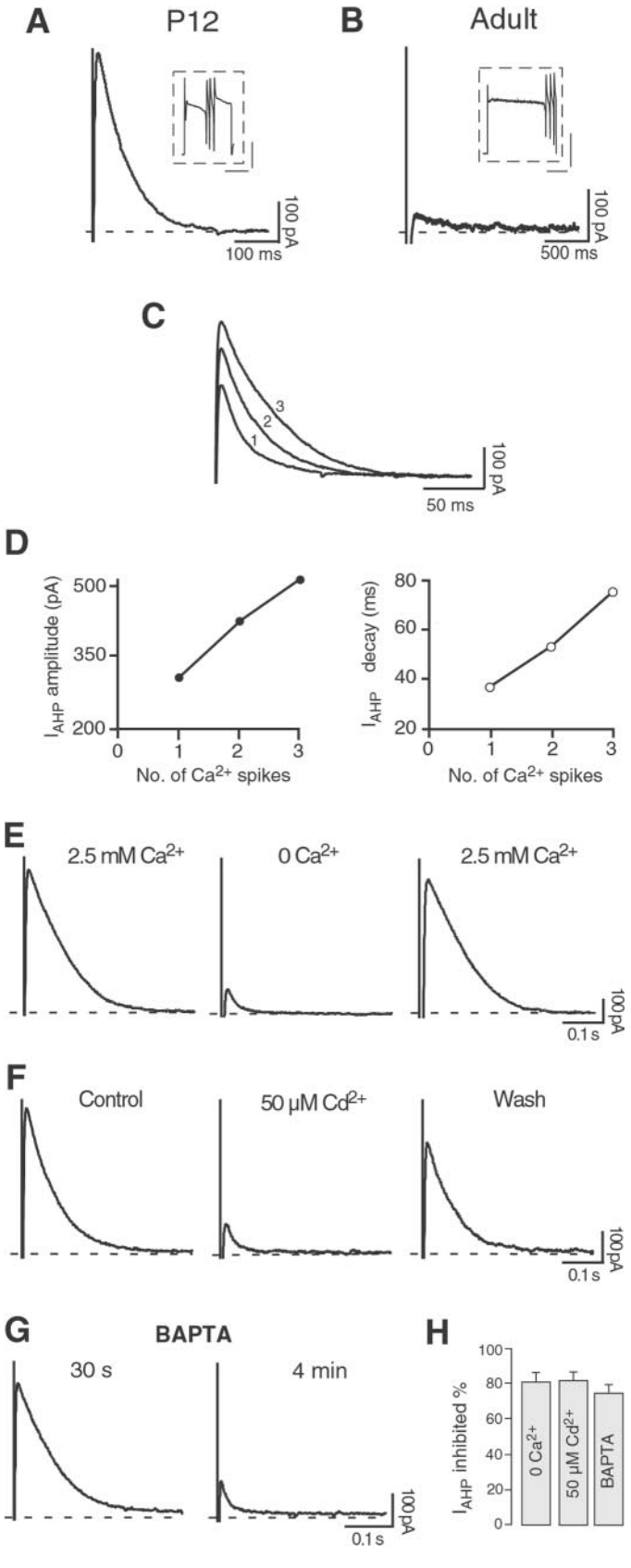

Figure 6. Purkinje neurons present a Ca^{2+}-activated K^+ current after depolarization-induced Ca^{2+} spikes at P12, but not at adult age under the same conditions. *A*, Tail current after a depolarizing pulse (200 msec to +10 mV) sufficient to elicit three Ca^{2+} spikes in a Purkinje cell at P12 in the presence of the Na^+ channel blocker TTX (0.5 μM) and of the BK channel blocker penitrem A (10 μM). A similar current was observed in nine cells. Calibration in *inset*: 1 nA, 100 msec. *B*, In an adult Purkinje cell, a longer depolarizing pulse (600 msec to −10 mV) was needed to elicit three Ca^{2+} spikes as in *A*, in the presence of identical concentrations of TTX and penitrem A. The Ca^{2+} influx did not induce a tail current as observed at P12. Similar results were obtained in four cells. Calibration in *inset*: 2 nA, 200 msec. *C*, *D*, The tail current amplitude and duration increased proportionally to the number of all-or-none Ca^{2+} spikes triggered by the depolarizing pulses. The *numbers* beside the current traces (*1*, *2*, *3*) indicate the number of Ca^{2+} spikes preceding each tail current. *E*, In P12 Purkinje cells, the tail current disappeared in Ca^{2+}-free medium (0 Ca^{2+}; 5 mM Mg^{2+}). This effect was fully reversible. *F*, The Ca^{2+} channel blocker Cd^{2+} (50 μM) strongly and reversibly suppressed the tail current. *G*, When the Ca^{2+} chelator BAPTA (10 mM) was enclosed in the pipette solution, the tail current was progressively reduced during the first minutes in the whole-cell configuration. *H*, Bar diagram summarizing the results presented in *E–G*. In Ca^{2+}-free medium the tail current was reduced by 81 ± 5% (n = 3); 50 μM Cd^{2+} suppressed the tail current by 82 ± 5% (n = 5). In the presence of BAPTA, the tail current was inhibited by 75 ± 5% (n = 4).

and Sugimori, 1979, 1980a,b), to our knowledge this is the first study investigating the ontogenesis, molecular basis, and function of the purely Ca^{2+}-activated SK channels in cerebellar neurons *in situ*. A developmental regulation has been described previously for the large conductance voltage- and Ca^{2+}-activated channel (BK) in primary cultures of Purkinje neurons (Yool et al., 1988; Muller et al., 1998). Interestingly, the ontogenetic pattern of BK channels is completely different from that of SK channels. Thus, BK channel expression increases gradually during the first 2 weeks of postnatal life and reaches high, stable levels in adult Purkinje neurons *in vivo* (Knaus et al., 1996; Muller et al., 1998). By contrast, *in situ* hybridization, immunohistochemistry, and electrophysiology provided convergent lines of evidence supporting the notion that SK channels of the SK2 type are highly expressed during the first 2–3 weeks of postnatal development and display a substantial downregulation in Purkinje neurons from P12 onwards. The other known members of the SK potassium channel subfamily, SK1 and SK3, are expressed neither in differentiating (this study) nor in adult Purkinje neurons (Stocker and Pedarzani, 2000).

The developmental pattern observed at the level of SK2 mRNA, protein, and corresponding AHP current was in good agreement with the results obtained in current-clamp recordings in P12 Purkinje neurons, where blockade of the SK channels by apamin favored the occurrence of spontaneous bursting and the transition from a silent to a spiking behavior (Fig. 4), whereas enhancement of SK channel activity by 1-EBIO converted bursting patterns into tonic, single-spiking ones (Fig. 5). Conversely, SK channel blockers did not display any effects on the spontaneous activity of adult Purkinje neurons, which were mainly silent under our recording conditions. Both the recording at room temperature and the removal of excitatory synaptic inputs by the slicing procedure (Llinas and Sugimori, 1980b) might have contributed to the decrease in spontaneous firing observed in our study. The lack of effect of apamin on the spontaneous firing of adult Purkinje cells reported in this study is in agreement with previous measurements performed in slices from adult guinea pig, where spontaneous spike doublets (measured in 5 mM extracellular K^+ at 30°C) were not affected by 1 μM apamin (Etzion and Grossman, 1998). In general, the changes in firing patterns observed in the presence of different SK channel modulators at P12 (Figs. 4, 5) were robust and reproducible, because they also persisted with identical features in perforated-patch or cell-

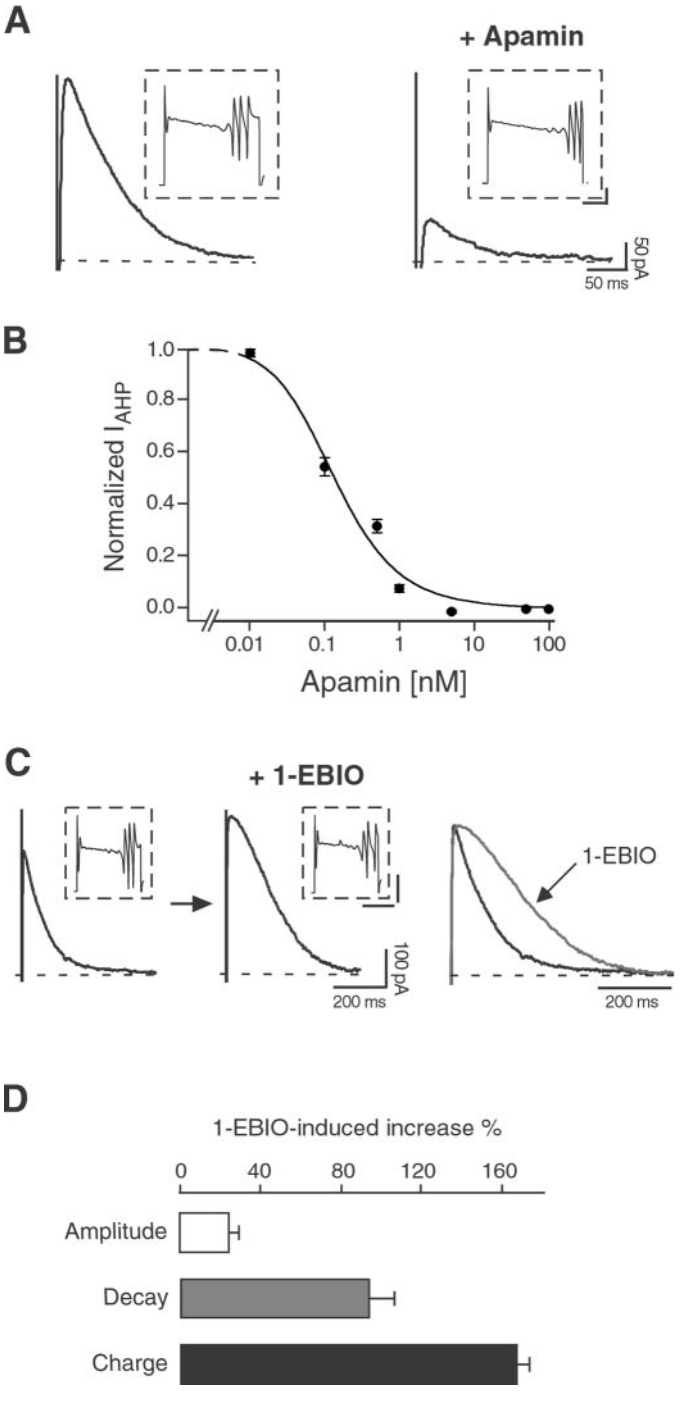

Figure 7. The Ca^{2+}-dependent tail current in P12 Purkinje neurons is an SK2-mediated I_{AHP}, sensitive to apamin and 1-EBIO. *A*, Apamin (50 nM) strongly and irreversibly suppressed I_{AHP}, without affecting the Ca^{2+} spikes elicited by the depolarizing pulses (*insets*), in Purkinje neurons at P12. Similar results were observed in 11 cells. Calibration in *insets*: 0.5 nA, 40 msec. *B*, Dose–response curve for the block of I_{AHP} by apamin. Data points were fit with the Hill equation, giving an IC_{50} value of ~135 pM and a Hill coefficient of 1. For each point, $n = 3–6$; error bars are SEM. *C*, 1-EBIO (100 μM) enhanced I_{AHP} in P12 Purkinje cells, without significantly affecting the Ca^{2+} spikes (*insets*). The *right panel* shows the two traces scaled and overlapped to display the effect of 1-EBIO on the time course of I_{AHP}. Similar effects were observed in five cells. Calibration in *insets*: 1 nA, 100 msec. *D*, Bar diagram summarizing the effects of 1-EBIO (100 μM) on I_{AHP}. The AHP current amplitude was increased by 25 ± 5%, the time constant of decay was increased by 95 ± 12%, and the total charge transfer was increased by 168 ± 6% ($n = 5$).

attached recordings. Apamin did not modify the spontaneous firing patterns of P12 Purkinje neurons by changing their membrane potential but rather by reducing the afterhyperpolarizing current activated by Ca^{2+} entering the neurons during single and bursts of action potentials.

Surprisingly, the presence of the apamin-sensitive current decreased rather than enhanced the hyperpolarization after each burst while slowing down the action potential firing to a modest rate within each burst (intraburst frequency) (Fig. 4*A*, *left panel*). The observed decrease in the hyperpolarization after each burst could be explained by the fact that in the presence of the AHP current the intraburst firing frequency was low, thus limiting the Ca^{2+} buildup and the accumulation of Na^+ channel inactivation that might contribute to the interburst hyperpolarization. The lack of contribution of the AHP current to the interburst hyperpolarization, as shown in this study, raises the question of which conductances underlie it. We have preliminary evidence that a Ca^{2+}-dependent current that is insensitive to apamin and to low concentrations of TEA is present in adult Purkinje cells (L. A. Cingolani, M. Stocker, and P. Pedarzani, unpublished observation). This current would fit in the model proposed by Pouille et al. (2000) in which the rhythmic interplay between low-threshold Ca^{2+} current and a calcium-dependent hyperpolarizing conductance would underlie the bursting firing pattern in Purkinje cells, but its contribution to the bursting firing pattern needs further investigation. Moreover, it is noteworthy that the results we obtained with apamin on the spontaneous firing of P12 Purkinje cells are comparable with the effect of this blocker on the endogenous firing pattern of deep cerebellar nuclei neurons at P12–15, where apamin also induced spontaneous, regularly occurring spike bursts (Aizenman and Linden, 1999). This finding is in agreement with the expression of the SK2 channel subunit that we observed also in deep cerebellar nuclei neurons at P12 (Figs. 1, 2).

The ability of immature Purkinje neurons to endogenously generate electrical activity has been documented in different preparations, including Purkinje cells in acutely isolated preparations (Nam and Hockberger, 1997; Raman and Bean, 1997, 1999), in primary culture (Gruol and Franklin, 1987; Gruol et al., 1991), and already starting from P2 *in vivo* (Woodward et al., 1969; Crepel, 1972). Besides endogenous conductances, such as sodium currents (Nam and Hockberger, 1997; Raman and Bean, 1997), excitatory and inhibitory synaptic inputs also contribute to the spontaneous activity of developing Purkinje neurons. In the acute slice preparation used in this study, the question arises whether the SK channels are localized exclusively postsynaptically or possibly also presynaptically. In our study the effect of apamin on the spontaneous firing of P12 Purkinje neurons is most likely attributable to a postsynaptic effect on SK channels, given their high expression in the Purkinje cell somata and main dendritic branches. Furthermore, no effects of apamin on the spontaneous firing pattern of Purkinje cells would be expected in the presence of GABA or glutamate receptor inhibitors if apamin acted on the spontaneous firing by affecting the release of GABA or glutamate from presynaptic terminals of interneurons or granule cells. Instead, when we suppressed synaptic signaling by application of glutamate and GABA receptor inhibitors, the enhancement of burst firing induced by apamin persisted (Cingolani, Stocker, and Pedarzani, unpublished data). Apamin has been reported not to block somatic potassium current in basket cells (Southan and Robertson, 1998, 2000) and not to affect axonal Ca^{2+} transients and neurotransmitter release from basket cell terminals (Tan and Llano, 1999). These results further support the view that a

presynaptic action of the toxin on GABAergic interneurons is unlikely to be responsible for the effects observed on the spontaneous firing of Purkinje neurons.

The *in situ* hybridization (Fig. 1) and immunohistochemistry results (Fig. 2) pointed to SK2 as the main channel underlying the effects of SK channel modulators on the firing properties of P12 Purkinje neurons. The pharmacological characterization of the AHP current that we performed on P12 Purkinje cells revealed an IC_{50} of I_{AHP} for apamin of 135 pM, close to those reported for homomultimeric SK2 channels in different expression systems (range, 27–83 pM) (Kohler et al., 1996; Strobaek et al., 2000; Grunnet et al., 2001). This result strongly supports the hypothesis that Purkinje cells express homomultimeric SK2 channels at early postnatal developmental stages. The downregulation of SK2 expression observed by *in situ* hybridization and immunohistochemistry was reflected by an absence of I_{AHP} in adult Purkinje cells after a triggering pulse comparable to the one used at P12. This result is in good agreement with the lack of effect of apamin on the spontaneous firing of adult Purkinje cells and with the absence of apamin-sensitive channels in nucleated patches from Purkinje neurons from 3- to 5-week-old mice, as reported by Southan and Robertson (2000).

The SK channel enhancer 1-EBIO has been shown in a previous work to increase the amplitude of the apamin-sensitive I_{AHP} in hippocampal pyramidal neurons two- to threefold (Pedarzani et al., 2001). The effect of 1-EBIO on I_{AHP} in Purkinje cells is different from the one observed in CA1 neurons. Thus, in Purkinje cells 1-EBIO affected only marginally the peak amplitude of I_{AHP} but strongly slowed down the decay time course of this current (Fig. 7*C*,*D*). The reason for this different effect lies in the mechanism of action of 1-EBIO on SK2 channels. In the presence of saturating Ca^{2+} concentrations (1–10 μM), the main effect of 1-EBIO is to slow down the deactivation of SK2 channels (Pedarzani et al., 2001), and the result obtained in Purkinje cells suggests that SK channels might be exposed to almost saturating $[Ca^{2+}]_i$ in response to the protocol used to elicit I_{AHP}. This assumption is in accord with the $[Ca^{2+}]_i$ measured during depolarizing pulses in Purkinje cell somata and dendrites and attained mean values of 5 and 30 μM (500 msec pulses) (Maeda et al., 1999) and ~2 and 4 μM (100 msec pulses) (Llano et al., 1994), respectively, and 0.5–1.5 μM in a somatic submembrane compartment (100 msec pulses) (Eilers et al., 1995). Similar Ca^{2+} transients were observed in the dendrites and in a narrow somatic submembrane shell in Purkinje cells during stimulation of climbing fibers (Eilers et al., 1995, 1996), suggesting that SK channels might respond and possibly regulate the Ca^{2+} signals elicited by synaptic activity.

Our results show that the postnatal change in the expression of SK2 channels parallels, on one hand, the development of the dendritic tree and the establishment of mature synaptic contacts onto Purkinje cells, which is completed by P21 (Altman and Bayer, 1997). On the other hand, it inversely correlates with the maturation of the Ca^{2+}-buffering properties of Purkinje neurons, because it has been shown that the Ca^{2+}-binding ratio doubles from P6 to P15 (Fierro and Llano, 1996), and this is most likely related to a developmentally regulated increase in the concentration of Ca^{2+}-binding proteins, such as parvalbumin and calbindin (Iacopino et al., 1990; Solbach and Celio, 1991). A recent study has additionally shown that spontaneous Ca^{2+} oscillations, mediated by L-type Ca^{2+} channels and elicited by endogenously generated electrical activity, are a prominent feature of early developing Purkinje neurons (Liljelund et al., 2000). Taking all this evidence into consideration, we propose that SK2 channels might play a pivotal role in the regulation of Ca^{2+} transients and oscillations during the first 2 weeks of postnatal development of Purkinje cells, whereas at later developmental stages a mature pattern of Ca^{2+} channels, BK channels, and Ca^{2+} buffering proteins might take over in regulating and shaping the Ca^{2+} signals generated by mature synapses.

REFERENCES

Aizenman CD, Linden DJ (1999) Regulation of the rebound depolarization and spontaneous firing patterns of deep nuclear neurons in slices of rat cerebellum. J Neurophysiol 82:1697–1709.

Altman J (1972) Postnatal development of the cerebellar cortex in the rat. II. Phases in the maturation of Purkinje cells and of the molecular layer. J Comp Neurol 145:399–463.

Altman J, Bayer SA (1997) Development of the cerebellar system in relation to its evolution, structure, and functions. Boca Raton, FL: CRC.

Ben-Ari Y (2001) Developing networks play a similar melody. Trends Neurosci 24:353–360.

Crepel F (1972) Maturation of the cerebellar Purkinje cells. I. Postnatal evolution of the Purkinje cell spontaneous firing in the rat. Exp Brain Res 14:463–471.

Eilers J, Callewaert G, Armstrong C, Konnerth A (1995) Calcium signaling in a narrow somatic submembrane shell during synaptic activity in cerebellar Purkinje neurons. Proc Natl Acad Sci USA 92:10272–10276.

Eilers J, Plant T, Konnerth A (1996) Localized calcium signalling and neuronal integration in cerebellar Purkinje neurones. Cell Calcium 20:215–226.

Etzion Y, Grossman Y (1998) Potassium currents modulation of calcium spike firing in dendrites of cerebellar Purkinje cells. Exp Brain Res 122:283–294.

Falk T, Muller YL, Yool AJ (1999) Differential expression of three classes of voltage-gated Ca^{2+} channels during maturation of the rat cerebellum in vitro. Brain Res Dev Brain Res 115:161–170.

Fierro L, Llano I (1996) High endogenous calcium buffering in Purkinje cells from rat cerebellar slices. J Physiol (Lond) 496:617–625.

Goldowitz D, Hamre K (1998) The cells and molecules that make a cerebellum. Trends Neurosci 21:375–382.

Grunnet M, Jensen BS, Olesen SP, Klaerke DA (2001) Apamin interacts with all subtypes of cloned small-conductance Ca^{2+}-activated K^+ channels. Pflügers Arch 441:544–550.

Gruol DL, Franklin CL (1987) Morphological and physiological differentiation of Purkinje neurons in cultures of rat cerebellum. J Neurosci 7:1271–1293.

Gruol DL, Jacquin T, Yool AJ (1991) Single-channel K^+ currents recorded from the somatic and dendritic regions of cerebellar Purkinje neurons in culture. J Neurosci 11:1002–1015.

Gruol DL, Deal CR, Yool AJ (1992) Developmental changes in calcium conductances contribute to the physiological maturation of cerebellar Purkinje neurons in culture. J Neurosci 12:2838–2848.

Hatten ME, Heintz N (1995) Mechanisms of neural patterning and specification in the developing cerebellum. Annu Rev Neurosci 18:385–408.

Hirschberg B, Maylie J, Adelman JP, Marrion NV (1999) Gating properties of single SK channels in hippocampal CA1 pyramidal neurons. Biophys J 77:1905–1913.

Iacopino AM, Rhoten WB, Christakos S (1990) Calcium binding protein (calbindin-D28k) gene expression in the developing and aging mouse cerebellum. Brain Res Mol Brain Res 8:283–290.

Joiner WJ, Wang LY, Tang MD, Kaczmarek LK (1997) hSK4, a member of a novel subfamily of calcium-activated potassium channels. Proc Natl Acad Sci USA 94:11013–11018.

Knaus HG, Schwarzer C, Koch RO, Eberhart A, Kaczorowski GJ, Glossmann H, Wunder F, Pongs O, Garcia ML, Sperk G (1996) Distribution of high-conductance Ca^{2+}-activated K^+ channels in rat brain: targeting to axons and nerve terminals. J Neurosci 16:955–963.

Kohler M, Hirschberg B, Bond CT, Kinzie JM, Marrion NV, Maylie J, Adelman JP (1996) Small-conductance, calcium-activated potassium channels from mammalian brain. Science 273:1709–1714.

Latham A, Paul DH (1971) Spontaneous activity of cerebellar Purkinje cells and their responses to impulses in climbing fibres. J Physiol (Lond) 213:135–156.

Liljelund P, Netzeband JG, Gruol DL (2000) L-type calcium channels mediate calcium oscillations in early postnatal Purkinje neurons. J Neurosci 20:7394–7403.

Llano I, DiPolo R, Marty A (1994) Calcium-induced calcium release in cerebellar Purkinje cells. Neuron 12:663–673.

Llinas R, Sugimori M (1979) Calcium conductances in Purkinje cell dendrites: their role in development and integration. Prog Brain Res 51:323–334.

Llinas R, Sugimori M (1980a) Electrophysiological properties of in vitro Purkinje cell dendrites in mammalian cerebellar slices. J Physiol (Lond) 305:197–213.
Llinas R, Sugimori M (1980b) Electrophysiological properties of in vitro Purkinje cell somata in mammalian cerebellar slices. J Physiol (Lond) 305:171–195.
Maeda H, Ellis-Davies GC, Ito K, Miyashita Y, Kasai H (1999) Supralinear Ca^{2+} signaling by cooperative and mobile Ca^{2+} buffering in Purkinje neurons. Neuron 24:989–1002.
Milosevic A, Zecevic N (1998) Developmental changes in human cerebellum: expression of intracellular calcium receptors, calcium-binding proteins, and phosphorylated and nonphosphorylated neurofilament protein. J Comp Neurol 396:442–460.
Miyakawa H, Lev-Ram V, Lasser-Ross N, Ross WN (1992) Calcium transients evoked by climbing fiber and parallel fiber synaptic inputs in guinea pig cerebellar Purkinje neurons. J Neurophysiol 68:1178–1189.
Muller YL, Yool AJ (1998) Increased calcium-dependent K^+ channel activity contributes to the maturation of cellular firing patterns in developing cerebellar Purkinje neurons. Brain Res Dev Brain Res 108:193–203.
Muller YL, Reitstetter R, Yool AJ (1998) Regulation of Ca^{2+}-dependent K^+ channel expression in rat cerebellum during postnatal development. J Neurosci 18:16–25.
Muller YL, Reitstetter R, Yool AJ (2000) Antisense knockdown of calcium-dependent K^+ channels in developing cerebellar Purkinje neurons. Brain Res Dev Brain Res 120:135–140.
Nam SC, Hockberger PE (1997) Analysis of spontaneous electrical activity in cerebellar Purkinje cells acutely isolated from postnatal rats. J Neurobiol 33:18–32.
Ni B, Rush S, Gurd JW, Brown IR (1992) Molecular cloning of calmodulin mRNA species which are preferentially expressed in neurons in the rat brain. Brain Res Mol Brain Res 13:7–17.
O'Donovan MJ (1999) The origin of spontaneous activity in developing networks of the vertebrate nervous system. Curr Opin Neurobiol 9:94–104.
Pedarzani P, Kulik A, Muller M, Ballanyi K, Stocker M (2000) Molecular determinants of Ca^{2+}-dependent K^+ channel function in rat dorsal vagal neurones. J Physiol (Lond) 527:283–290.
Pedarzani P, Mosbacher J, Rivard A, Cingolani LA, Oliver D, Stocker M, Adelman JP, Fakler B (2001) Control of electrical activity in central neurons by modulating the gating of small conductance Ca^{2+}-activated K^+ channels. J Biol Chem 276:9762–9769.
Pouille F, Cavelier P, Desplantez T, Beekenkamp H, Craig PJ, Beattie RE, Volsen SG, Bossu JL (2000) Dendro-somatic distribution of calcium-mediated electrogenesis in Purkinje cells from rat cerebellar slice cultures. J Physiol (Lond) 527.2:265–282.
Raman IM, Bean BP (1997) Resurgent sodium current and action potential formation in dissociated cerebellar Purkinje neurons. J Neurosci 17:4517–4526.
Raman IM, Bean BP (1999) Ionic currents underlying spontaneous action potentials in isolated cerebellar Purkinje neurons. J Neurosci 19:1663–1674.
Regan LJ (1991) Voltage-dependent calcium currents in Purkinje cells from rat cerebellar vermis. J Neurosci 11:2259–2269.
Ribera AB (1999) Potassium currents in developing neurons. Ann NY Acad Sci 868:399–405.
Sah P (1996) Ca^{2+}-activated K^+ currents in neurones: types, physiological roles and modulation. Trends Neurosci 19:150–154.
Schwindt PC, Spain WJ, Crill WE (1992) Calcium-dependent potassium currents in neurons from cat sensorimotor cortex. J Neurophysiol 67:216–226.
Solbach S, Celio MR (1991) Ontogeny of the calcium binding protein parvalbumin in the rat nervous system. Anat Embryol 184:103–124.
Southan AP, Robertson B (1998) Patch-clamp recordings from cerebellar basket cell bodies and their presynaptic terminals reveal an asymmetric distribution of voltage-gated potassium channels. J Neurosci 18:948–955.
Southan AP, Robertson B (2000) Electrophysiological characterization of voltage-gated K^+ currents in cerebellar basket and Purkinje cells: Kv1 and Kv3 channel subfamilies are present in basket cell nerve terminals. J Neurosci 20:114–122.
Spilker C, Richter K, Smalla KH, Manahan-Vaughan D, Gundelfinger ED, Braunewell KH (2000) The neuronal EF-hand calcium-binding protein visinin-like protein-3 is expressed in cerebellar Purkinje cells and shows a calcium-dependent membrane association. Neuroscience 96:121–129.
Spitzer NC (1994) Spontaneous Ca^{2+} spikes and waves in embryonic neurons: signaling systems for differentiation. Trends Neurosci 17:115–118.
Spitzer NC, Ribera AB (1998) Development of electrical excitability in embryonic neurons: mechanisms and roles. J Neurobiol 37:190–197.
Spitzer NC, Gu X, Olson E (1994) Action potentials, calcium transients and the control of differentiation of excitable cells. Curr Opin Neurobiol 4:70–77.
Stocker M, Pedarzani P (2000) Differential distribution of three Ca^{2+}-activated K^+ channel subunits, SK1, SK2, and SK3, in the adult rat central nervous system. Mol Cell Neurosci 15:476–493.
Stocker M, Krause M, Pedarzani P (1999) An apamin-sensitive Ca^{2+}-activated K^+ current in hippocampal pyramidal neurons. Proc Natl Acad Sci USA 96:4662–4667.
Strehler EE, Zacharias DA (2001) Role of alternative splicing in generating isoform diversity among plasma membrane calcium pumps. Physiol Rev 81:21–50.
Strobaek D, Jorgensen TD, Christophersen P, Ahring PK, Olesen SP (2000) Pharmacological characterization of small-conductance Ca^{2+}-activated K^+ channels stably expressed in HEK 293 cells. Br J Pharmacol 129:991–999.
Strong PN (1990) Potassium channel toxins. Pharmacol Ther 46:137–162.
Takei K, Stukenbrok H, Metcalf A, Mignery GA, Sudhof TC, Volpe P, De Camilli P (1992) Ca^{2+} stores in Purkinje neurons: endoplasmic reticulum subcompartments demonstrated by the heterogeneous distribution of the InsP3 receptor, Ca^{2+}-ATPase, and calsequestrin. J Neurosci 12:489–505.
Tan YP, Llano I (1999) Modulation by K^+ channels of action potential-evoked intracellular Ca^{2+} concentration rises in rat cerebellar basket cell axons. J Physiol (Lond) 520:65–78.
Tank DW, Sugimori M, Connor JA, Llinas RR (1988) Spatially resolved calcium dynamics of mammalian Purkinje cells in cerebellar slice. Science 242:773–777.
Uzman LL (1960) The histogenesis of the mouse cerebellum as studied by its tritiated thymidine uptake. J Comp Neurol 114:137–159.
Wolfart J, Neuhoff H, Franz O, Roeper J (2001) Differential expression of the small-conductance, calcium-activated potassium channel SK3 is critical for pacemaker control in dopaminergic midbrain neurons. J Neurosci 21:3443–3456.
Woodward DJ, Hoffer BJ, Lapham LW (1969) Postnatal development of electrical and enzyme histochemical activity in Purkinje cells. Exp Neurol 23:120–139.
Xia XM, Fakler B, Rivard A, Wayman G, Johnson-Pais T, Keen JE, Ishii T, Hirschberg B, Bond CT, Lutsenko S, Maylie J, Adelman JP (1998) Mechanism of calcium gating in small-conductance calcium-activated potassium channels. Nature 395:503–507.
Yool AJ, Dionne VE, Gruol DL (1988) Developmental changes in K^+-selective channel activity during differentiation of the Purkinje neuron in culture. J Neurosci 8:1971–1980.